ATOMIC BEAM FREQUENCY STANDARDS

BY

R. C. MOCKLER, R. E. BEEHLER, AND C. S. SNIDER

Reprinted from IRE TRANSACTIONS
ON INSTRUMENTATION
Volume I-9, Number 2, September, 1960

PRINTED IN THE U.S.A.

Atomic Beam Frequency Standards*

R. C. MOCKLER†, R. E. BEEHLER†, AND C. S. SNIDER†

I. Introduction

THE separations of the quantum states of a completely isolated atom or molecule are expected to be fixed in time. The measurement of one of these separations by a suitable measuring apparatus would provide, one would suppose, a very excellent standard of frequency and time. Nevertheless, the presence of a measuring apparatus introduces an uncertainty in the measurements, since the atomic or molecular system is no longer isolated. Furthermore, a measurement usually requires many atoms or molecules that are mutually perturbing. The most exact measurement of the quantum state separation is obtained when the apparatus and the particles interact to the least degree which is consistent with a reasonable signal-to-noise ratio. Certain kinds of perturbations incurred by the apparatus can be calculated and compensated for. These are not to be considered undesirable, and frequently they are essential to the observations.

The most precise measurements of quantum state separations can be made for those energy levels in the ground electronic state of atoms and molecules.

The atomic beam magnetic resonance technique provides a method of measuring the state separations, and it introduces the smallest perturbation on the atomic system of the presently known techniques. Furthermore, it is probably better understood than other methods.

The same can be said of the molecular beam technique, but certain atomic transitions have significant advantages in intensity over molecular transitions in beam experiments.

For the purpose of a standard of frequency and time it is important to choose a transition of high frequency, which is within the reach of existing coherent radiators, and of high intensity (for the sake of precision in measurement). There are other practical difficulties that must also be taken into account.

At the present time the $(F=4,\ m_F=0)\leftrightarrow(F=3,\ m_F=0)$ transition between the two hyperfine structure levels in cesium is used exclusively in atomic beam frequency standards.[1]

The problem of eliminating systematic errors in atomic beam frequency standards is a difficult one. It is of special concern because at the present time these instrumental errors limit the absolute accuracy of the devices. These errors are evident in experiments comparing different cesium beam standards. Such comparisons have been made by a number of laboratories. Those comparisons between devices in the same laboratory, rather than through propagation data, are of particular interest [2]-[4].

The results of Holloway, *et al.* [2], showed agree-

* Received by the PGI, June 22, 1960. Presented at the 1960 Conference on Standards and Electronic Measurements as paper 2-1.
† National Bureau of Standards, Boulder, Colo.

[1] The hyperfine transition in thallium may provide an even better standard [1].

ment to about 2×10^{-10} (after certain corrections) between the commercial beam standards developed and manufactured by the National Company and the atomic standard at the National Physical Laboratory, Teddington, England.

Over the last several months, comparisons have been made between two dissimilar cesium beam standards constructed at the National Bureau of Standards. Particular care was taken to avoid systematic errors. The devices were tested independently, the pertinent parameters were measured, and the frequency comparisons were subsequently made.

The zero field frequencies of these two standards agree to a fixed difference of 1×10^{-11}. The standard deviation of the mean of the difference frequency is 2×10^{-12}. This latter number represents the precision of measurement for measuring times of a few hours. The accuracy of these standards is considered to be $\pm1.5\times10^{-11}$, taking into account certain uncertainties in the C-field measurements.

This report has eight sections. The Introduction is followed by a brief description, Sections II and III, of an atomic beam experiment and of the kind of spectrum upon which the standard is based. Section IV describes in some detail the features peculiar to the National Bureau of Standards machines, the method of measurement and the various tests performed to determine accuracy and precision. Section V includes frequency comparisons between the two Bureau standards and atomic beam standards elsewhere in the United States, Canada and England. Section VI very briefly discusses other types of atomic frequency standards. Sections VII and VIII contain some concluding remarks and the acknowledgments.

II. Theory—Descriptive

For many years, physicists have used atomic beam techniques to investigate the detailed features of atomic spectra [5]. These same techniques, with, perhaps, some embellishments, are used in atomic beam frequency standards.

A. Atomic Hyperfine Structure

The quantum transitions employed in present-day atomic beam standards occur between the hyperfine levels in the ground state of the alkali metals. This hyperfine splitting of the ground state arises because of the interaction between the magnetic moment of the nucleus and magnetic field produced by the valence electron at the position of the nucleus.

The potential energy of the nuclear magnet in this field depends upon its orientation in the field. Simply, it is given by

$$W = -\boldsymbol{\mu}_I \cdot \boldsymbol{H}_{el}, \tag{1}$$

where $\boldsymbol{\mu}_I$ is the magnetic dipole moment of the nucleus and $\boldsymbol{H}_{el}$ is the magnetic field intensity at the nucleus produced by the valence electron. If an external field is applied, it will interact with the electron and the nucleus, resulting in a change in the energy W.

By pursuing the problem in the framework of the quantum theory, the various possible energy states of the atom are obtained. It will have a different energy state for every possible orientation of the nucleus for a given electronic configuration.

The total angular momentum of the atom, usually designated by $\boldsymbol{F}$, is the vector sum of the nuclear spin angular momentum $\boldsymbol{I}$, and the angular momentum of the electron $\boldsymbol{J}$. Associated with each of these angular momenta is a quantum number F, I, and J, respectively. The possible values of the total angular momentum quantum number F are

$$F = (I + J), (I + J - 1), \cdots, (I - J)$$

if $I>J$, and

$$F = (J + I)(J + I - 1), \cdots, (J - I)$$

if $J>I$. For cesium (133), $I=7/2$ and $J=\frac{1}{2}$ for the ground state, and F has the two possible values 3 and 4. These two states are separated in zero applied field by 9192.631 $\cdots$ Mc. The upper energy state for which $F=4$ is split into nine levels if an external magnetic field is applied, and the $F=3$ state is split into seven different levels. An F state is said to be $2F+1$ fold degenerate in zero field. (See Fig. 1.)

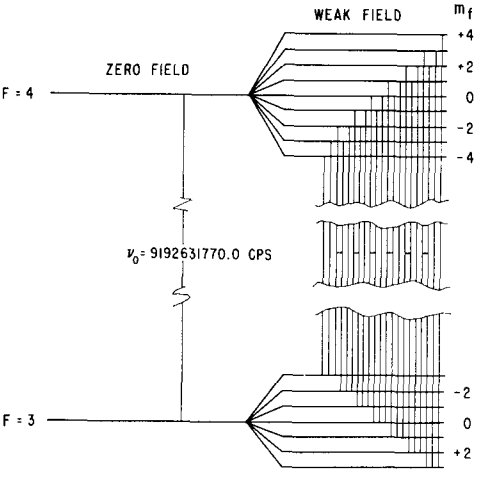

Fig. 1—Energy level diagram for Cs^{133}. $I=7/2$, $J=1/2$, positive nuclear moment selection rules $\Delta F=0, \pm1$; $\Delta m_F=0, \pm1$.

The transition between the upper level for which $F=4$, $m_F=0$ and the lower level for which $F=3$, $m_F=0$ is the transition that has been adopted as the standard of frequency.

In emission, a quantum of energy $h\nu_0'$ is emitted and in absorption, a quantum $h\nu_0'$ is absorbed, where

$$\nu_0' = \nu_0 + 427H_0^2. \tag{2}$$

In (2), ν_0' and ν_0 are frequencies measured in cycles per

second, and H_0 is a small externally applied magnetic field measured in oersteds. The coefficient of H_0^2 is peculiar to this particular cesium (133) transition.

It is interesting to note that this type of transition in the alkali metals corresponds to the more familiar 1420-Mc transition between the hyperfine levels of atomic hydrogen of so much importance in radio astronomy.

B. The Atomic Beam Spectrometer

Uniform magnetic or electric fields only exert a torque on a dipole; they deflect only charged particles. On the other hand, a nonuniform field applies both a torque and a resultant force on a dipole. The deflection of a beam of neutral particles by an inhomogeneous magnetic field was first studied by Stern and Gerlach. Their original celebrated experiments led to the very precise methods of present-day atomic and molecular beam spectroscopy.

A schematic of a typical spectrometer used in atomic beam resonance experiments is shown in Fig. 2(a) and 2(b). Many variations exist in atomic beam design. The design discussed here is that used in the Bureau frequency standards.

Neutral atoms effuse from the oven in the left of the figure and pass through the nonuniform magnetic field of the A magnet. The atoms have a magnetic dipole moment and, consequently, have a transverse force acting upon them in this nonuniform field. The magnitude of this force depends upon which of the states (see Fig. 1) the particular atom in question is in. Some of the atoms have their trajectories bent toward the axis (see Fig. 2) and cross the axis at the position of the collimator slit. The field of the B magnet is identical to that of the A magnet. Therefore, in this field, the forces on the atoms tend to give them trajectories diverging from the axis, since they cross the axis at the collimator slit and the force is in the same direction as it is in magnet A. However, if the atoms are subjected to a radiation field of just the proper frequency, ν_0', the magnetic moment of the atom is "flipped" to a direction opposite to its original one. Since the sign of the magnetic moment has changed in moving from the A magnet to the B magnet, the force on the atom reverses its direction, and the atom is refocused onto the axis at the detector. Thus, as the frequency of the radiation is swept through ν_0', the detected signal increases and reaches a maximum when $\nu=\nu_0'$ and then decreases as the radiation frequency is varied beyond ν_0'.

The discussion can be made more quantitative rather simply. Suppose the energy of an atom in the beam is designated by $W(H)$. We suppose the field to be conservative so that the force on the atom is given by

$$\boldsymbol{F} = -\nabla W.^2 \tag{3}$$

[2] Here $\boldsymbol{F}$ is the force vector and is not to be confused with the previous $\boldsymbol{F}$ which represented the total angular momentum vector of the atom.

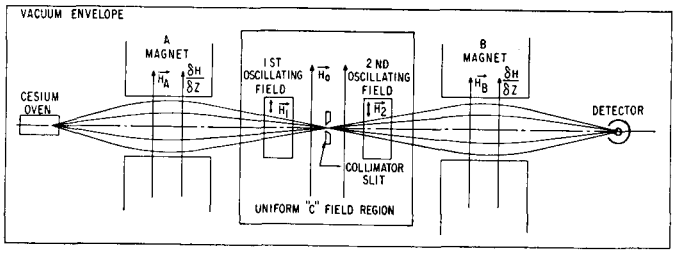

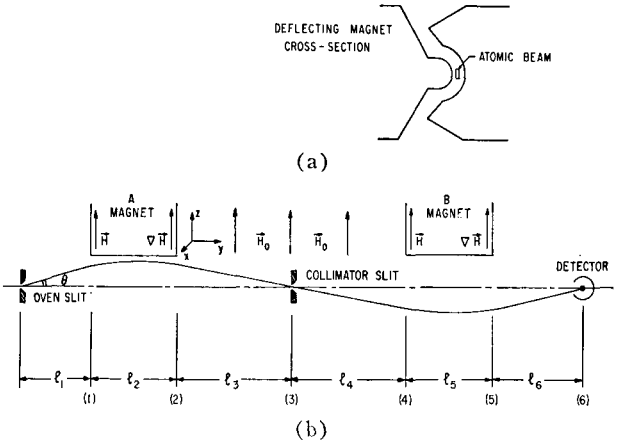

Fig. 2—(a) A schematic of a typical atomic beam spectrometer. The indicated trajectories are for atoms that make transitions. (b) The trajectory of a single atom leaving the source at an angle θ and with a particular speed v.

This can be rewritten as

$$\boldsymbol{F} = -\frac{\partial W}{\partial H}\nabla H, \tag{4}$$

provided that the only dependence on position that W has is through the spatial variation of the magnetic field intensity H. Note that $\boldsymbol{F}$ is different from zero only when the field has a gradient which is different from zero, *i.e.*, when the field is nonuniform, and when W depends upon H. The Breit-Rabi formula provides the proper form for W for the case $J=\frac{1}{2}$ [5]. The partial derivative, $-(\partial W/\partial H)$ is called the effective magnetic dipole moment μ_{eff}, then

$$\boldsymbol{F} = \mu_{\text{eff}}\nabla H. \tag{5}$$

The A and B deflecting magnets are designed such that the field configuration has a simple calculable form, and so that the force has the simple form

$$F_z = -\frac{\partial W}{\partial H}\frac{\partial H}{\partial z} = \text{constant}.$$

$$\ddot{z} = a = \frac{\mu_{\text{eff}}}{m}\frac{\partial H}{\partial z}. \tag{6}$$

The acceleration imparted to the atom in a direction transverse to the axis of the spectrometer is a, and m is the mass of the atom. It will be assumed that z is positive above the axis (center line of the beam) and negative below. [See Fig. 2(b).]

The acceleration a is different from zero only in regions 2 and 5, where the magnetic field is nonuniform.

Integration of the familiar differential (5) yields

$$\dot{z} = v_z = v_{zi} + at \tag{7}$$

and

$$z = z_i + v_{zi}t + \tfrac{1}{2}at^2, \tag{8}$$

where v_{zi} is the transverse velocity that the atom already has upon entering the deflecting field region, z_i is the z coordinate that the particle has as it enters this region, and t is the time spent in the given deflecting field region.

Atoms effuse from the source slit in all forward directions. Suppose an atom enters region 2 with a certain positive transverse velocity v_{z1} where $v_{z1}=v\sin\theta\approx v\theta$.[3] The speed of the atom as it leaves the oven is v. If a is negative for this atom, it is deflected toward the axis. Evidently this occurs if μ_{eff} is negative [see (7)]. μ_{eff} is negative for atoms in certain states. This is true of states for which $m_J=+\frac{1}{2}$ (electron spin "up"). These atoms pass through the collimator slit at position 3 for a particular angle θ (given $\partial H/\partial z$). If these atoms pass through the collimator slit, they enter the second deflecting region, 5, with a negative transverse velocity. Now all three terms of (7) are negative, and the particles are deflected further from the center line. If, however, the μ_{eff} is reversed in sign, by the application of an electromagnetic field of the proper frequency ν_0' in regions 3 and 4, refocusing onto the detector occurs.

If one proceeds with the analysis using (7), calculates the transverse displacement at each of the positions (1 through 6), and imposes the condition that $z_3=0$, the deflection at the detector plane z_6 is found to be

$$z_6 = \frac{1_5(1_5+21_6)}{2mv^2}\left[(\mu_{\text{eff}})_2+(\mu_{\text{eff}})_5\right]\frac{\partial H}{\partial z}. \tag{9}$$

It has been assumed for this calculation that the spectrometer is symmetric about the collimator slit, *i.e.*,

$$1_1 = 1_6,$$
$$1_2 = 1_5,$$
$$1_3 = 1_4,$$

and

$$\left(\frac{\partial H}{\partial z}\right)_2 = \left(\frac{\partial H}{\partial z}\right)_5.$$

If no radiation is applied, $(\mu_{\text{eff}})_2=(\mu_{\text{eff}})_5$. When radiation of frequency ν_0' is applied, $(\mu_{\text{eff}})_2=-(\mu_{\text{eff}})_5$, and refocusing occurs ($z_6=0$). An increase in the detector signal results.

Both the emission and absorption of radiation occur in the transition region between the A and B magnets when the frequency of the oscillating field is ν_0'.

The spectral line widths observed are given, approximately, by the uncertainty relation

$$\Delta E\Delta t \geqq h,$$

or

$$\Delta\nu\Delta t \geqq 1, \tag{10}$$

where $\Delta\nu$ is the line breadth, and Δt is the mean transit time of the atoms through the radiation field.

Low-frequency transitions between the m_F states of a given F level, $(F=4,\ m_F+1)\leftrightarrow(F=4,\ m_F)$ and $(F=3,\ m_F+1)\leftrightarrow(F=3,\ m_F)$, can also be induced by irradiating the beam with frequency ν_L, where

$$\nu_L(\mp) = 3.50\times10^5H_0 \mp 561H_0 - 26.7(m_F+\tfrac{1}{2})H_0^2.$$

In this equation the $(-)$ sign refers to transitions within the $F=4$ levels, and the $(+)$ sign refers to transitions within the $F=3$ levels. $\nu_L(\mp)$ is measured in cps and H_0 in oersteds.

The uniform field $\boldsymbol{H}_0$ (the C field) is essential in beam experiments, in order to preserve the state identity of the atom as it progresses through the apparatus. Transitions can occur in accordance with the selection rules $\Delta F=0,\pm1$ and $\Delta m_F=0,\pm1$.[4]

III. A Classical Description of the Excitation Process

The original (Rabi) method of exciting the atomic transitions in an atomic beam resonance experiment employs a single oscillating field. In 1950, Ramsey introduced a method by which the transitions are induced by two separated oscillating fields. There are a number of advantages to this method over the Rabi method. It improves the resolution of the spectrometer. It does not require as high a degree of uniformity of the static C field. It has a practical advantage in observing very high frequency transitions. The oscillating field must be uniform in intensity and phase, and this is a difficult situation to achieve when the oscillating field region is many free space wavelengths long. Two small oscillating fields separated by a distance L provide even higher resolution than a single field covering the entire distance L. This advantage is gained at the expense of a reduction in the signal-to-noise ratio.

A physical picture of the emission and absorption process can be gained from a classical description. (See Kusch and Hughes [5].)

A. The Rabi Method

First consider the simpler Rabi resonance method which employs a single oscillating field, and suppose that we examine the transition for an atom with spin $\frac{1}{2}$, since this is amenable to a classical description. The system consists of the uniform C field $\boldsymbol{H}_0$, the atom with

[3] The angle θ will always be very tiny for any atom that reaches the detector plane. Hence, $\sin\theta\sim\theta$ to a very good approximation.

[4] Multiple quantum jumps occur with lower probability and are disregarded.

angular momentum F moving with uniform velocity through H_0 and perpendicular to it, and an oscillating field also perpendicular to H_0 (Fig. 3).

The magnetic moment of the atom makes an angle θ with the Z axis, and the angular momentum makes an angle $\pi-\theta$ with the Z axis. In the absence of the oscillating field, μ precesses about H_0 with the Lamor frequency $\nu_0'=\mu H_0/F$, where F is the magnitude of the angular momentum. The time dependent field oscillating in the x-y plane can be considered the resultant of two rotating fields, each rotating uniformly about the Z axis with frequency ν in the X-Y plane but in opposite directions to each other. Call these two rotating fields H_1 and H_1'. The application of the rotating field H_1, with frequency $\nu\neq\nu_0'$, produces a torque, $\mu\times H_1$, which sometimes tends to increase the angle θ and sometimes tends to decrease it. As long as ν and ν_0' are widely different from each other, this torque produces a fast nutation of θ, that, on the average, produces no change in θ. When ν approaches ν_0', the rotating field that rotates in phase with the precession of μ, *e.g.*, H_1, has an appreciable effect on the angle θ. Suppose $\nu=\nu_0'$. Consider a coordinate system fixed to H_1 and rotating with it in phase with the precession of μ. There is a torque on μ in the rotating coordinate system that causes μ to precess about H_1. This slow precession increases the angle θ to θ' for example [Fig. 3(b)]. In the original stationary coordinate system the cone of precession opens and inverts periodically, *i.e.*, μ describes, at resonance, a helical motion downward and upward. For the particular situation (spin $\frac{1}{2}$) shown in Fig. 3, the angle formed with the Z axis varies for θ to $\pi-\theta$, periodically. The effect produced by the second component of the rotating field, rotating in the opposite direction to H_1 and out of phase with μ, can be ignored, because it produces only a rapid nutation of μ about Z.[5] At the resonant frequency, the magnetic moment can have its orientation relative to H_0 changed with the highest probability. This change in orientation of μ in the classical picture corresponds to a transition between two different energy states in quantum mechanics.

This classical description of the transition process can be worked out quantitatively, and the results agree with the quantum mechanical results for spin $\frac{1}{2}$. For the more complex situation of cesium there is no satisfactory classical treatment. Nevertheless, qualitatively, we may picture the process in the following way for the low-frequency transitions:

The various possible m_F states correspond to different angles θ between the angular momentum vector F (and, consequently, μ) and H_0. Suppose the atom to be in a particular state m_F with corresponding precessional angle θ_1, and consider a transition to the adjacent state m_F-1 with corresponding angle θ_2. The transition $(F, m_F)\rightarrow(F, m_F-1)$ corresponds to a change in the angle from θ_1 to θ_2 instead of a complete inversion, as in the case of spin $\frac{1}{2}$.

[5] The effect of H_1' can only be ignored when the precessional frequency is large, relative to the line width. The effect on some of the low-frequency measurements discussed later, in connection with the measurements of the C field, may be appreciable.

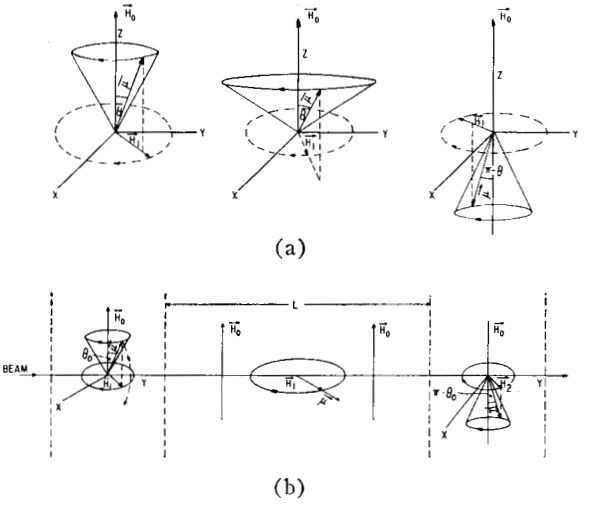

Fig. 3—A classical picture of the reorientation of the magnetic moment that occurs in the emission and absorption process. Transition induced by (a) a single oscillating field and (b) a double oscillating field.

B. The Ramsey Method

Consider now transitions induced by two oscillating field regions, separated by a distance L [Fig. 3(c)], again for spin $\frac{1}{2}$. There is a uniform field H_0 throughout the entire region. As an atom enters the first oscillating field, a torque is exerted by the rotating field H_1. If H_1 rotates in unison with the precession of μ about H_0, reorientation of the magnetic moment occurs. The magnitude of H_1 can be adjusted so that θ increases to $\pi/2$ in the time that the atom spends in the first field. Thus, as the atom enters the region between the two oscillating fields, it is precessing in the X-Y plane (still at the Larmor frequency). Upon entering the second oscillating field region a torque, $\mu\times H_2$, is applied in addition to $\mu\times H_0$. If H_2 is in phase with H_1, and if H_0 is uniform, H_2 rotates in unison with the precessional motion of μ about H_0. In the rotating system μ precesses slowly about H_2. In the fixed system, the cone of precession opens up from $\theta=\pi/2$ to $\theta=\pi-\theta_0$. Thus, the transition which corresponds to the reorientation of μ from an angle θ_0 to $\pi-\theta_0$ has been induced by the two oscillating fields together. If ν and ν_0' are slightly different, so that the relative phase angle between the rotating field vector and the precessing magnetic moment has changed by 180° in the time that it takes the atom to go from field H_1 to field H_2, the second field has the opposite effect to the first one, and θ is returned to θ_0. No transition occurs, and a minimum signal is observed. When the relative phase is an integral multiple of 360°, other signal maxima will be observed, giving the characteristic Ramsey pattern. The maximum for which $\nu=\nu_0'$ is of greatest intensity because of the velocity distribution of the atoms. In the case where $\nu=\nu_0'$, the phase of the rotating field and the magnetic

moment are independent of the velocity of the atom. The other cases, where ν and ν_0' differ such that a phase difference of some integer multiple of 360° accumulates, they are dependent upon the velocity. Slower molecules spend more time in going from the first to the second oscillating field, and a larger phase shift accumulates than for faster molecules. One then expects that more atoms make the transition at the resonance frequency. If a univelocity beam were employed, then the maxima would have nearly the same intensity near $\nu=\nu_0'$.

An argument similar to that given for the Rabi method for $F>\frac{1}{2}$ can be applied to describe the Ramsey transition process for cesium.

The discussion up to this point applies only to transitions between m_F levels for a given F, or the low-frequency transitions mentioned previously. These transitions are excited by radiation polarized perpendicular to the applied field $\boldsymbol{H}_0$. They are called π transitions, and the selection rule that applies is $\Delta m_F=\pm 1$. In the cesium frequency standard, the low frequency transitions are measured for the purpose of accurately measuring the magnitude of $\boldsymbol{H}_0$.[6]

The microwave frequency transitions occur between an m_F level in the $F=4$ state and another m_F level in the $F=3$ state. The field insensitive transition ($F=4$, $m_F=0$)↔($F=3$, $m_F=0$) is used as the standard of frequency. The selection rules are that $\Delta F=\pm 1$ and $\Delta m_F=0$. Transitions of this type ($\Delta m_F=0$) occur when there is a magnetic component of the radiation field parallel to the static field $\boldsymbol{H}_0$. They are called σ transitions.

The vector diagram for cesium (133) is shown in Fig. 4(a). The total angular momentum $\boldsymbol{F}$ and the vector sum of $\boldsymbol{I}$ and $\boldsymbol{J}$ precesses slowly about the static field direction at an angle depending upon the m_F state. Both $\boldsymbol{I}$ and $\boldsymbol{J}$ precess rapidly about $\boldsymbol{F}$. The magnetic moment $\boldsymbol{\mu}_J$ associated with $\boldsymbol{J}$ (and hence, with the electron) points in a direction opposite to $\boldsymbol{J}$ because of negative charge of electrons. It is much larger than $\boldsymbol{\mu}_I$, the magnetic moment associated with the nucleus, which has the same direction as $\boldsymbol{I}$. As a consequence, the resultant of $\boldsymbol{\mu}_I$ and $\boldsymbol{\mu}_J$, *i.e.*, $\boldsymbol{\mu}$, does not have its direction along $\boldsymbol{F}$. Since $\boldsymbol{I}$ and $\boldsymbol{J}$ precess rapidly about $\boldsymbol{F}$, so does $\boldsymbol{\mu}$. It is this rapid precession of $\boldsymbol{\mu}$ about $\boldsymbol{F}$ that must be considered in a classical description of the high-frequency transition. It must be emphasized, however, that the physical picture has now become more obscure and the mechanism of quantum mechanics is essential to a proper description.

The slow precession of $\boldsymbol{F}$ about $\boldsymbol{H}_0$ will be ignored for our descriptive purposes. The rate of this precession is much slower than the precessional rate of $\boldsymbol{\mu}$ about $\boldsymbol{F}$.[7]

In the standard frequency transition, $m_F=0$ in both the $F=3$ and $F=4$ states. For this particular value of m_F, the vector $\boldsymbol{F}$ is perpendicular to $\boldsymbol{H}_0$. We may now consider the reorientation of the precessing magnetic moment $\boldsymbol{\mu}$ by the application of a rotating field vector $\boldsymbol{H}_1$, which rotates in a plane perpendicular to $\boldsymbol{F}$. When $\boldsymbol{H}_1$ (the microwave field) rotates in unison with the precessional motion of $\boldsymbol{\mu}$, the magnetic moment inverts, and the previous arguments apply in a qualitative way. [See Fig. 4(b).]

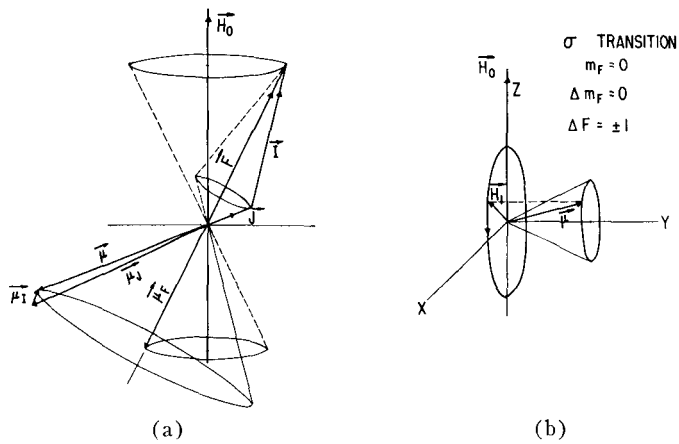

(a) (b)

Fig. 4—(a) The vector diagram of an atom with positive nuclear moment (not drawn to scale). (b) A classical picture of the transition process corresponding to a σ transition for $m_F=0$.

IV. Characteristic Features and the Performance of the Bureau Standards

A. Characteristics of the Beam Devices

The Bureau standards are shown in Figs. 5 and 6. These machines employ Ramsey-type excitation. The separation of the oscillating fields is 55 cm in the shorter machine (which is designated as NBS-I, Fig. 5), and the oscillating field separation is 164 cm in the longer machine (which is designated as NBS-II, Fig. 6). The source slit dimensions are 0.003 inch×0.100 inch and 0.015 inch×0.187 inch, respectively. The spectral line widths are 300 cps (NBS-I) and 120 cps (NBS-II) at the present time. These are the line widths for which greatest signal-to-noise is available and are not the narrowest attainable. The rather broad line for NBS-II, considering the interaction length, results apparently from cutting off some of the slow atoms of the velocity distribution by the small holes through the resonant cavity. The ends of this cavity were actually designed for NBS-I where the beam deflections are smaller. Enlarging these holes should reduce the optimum line width and increase the signal-to-noise ratio.

Hot wire detectors (20 per cent iridium—80 per cent platinum alloy) are used in conjunction with conventional electrometer circuits. Typical signal-to-noise ratios are about 400 for NBS-I and 100 for NBS-II. The oven temperature is 150°C for both.

The uniform C field ($\boldsymbol{H}_0$) is produced by passing a direct current of about one ampere through a conducting sector of a cylindrical brass tube contained within a

[6] Certain microwave transitions which provide a better measurement of H_0 are also used.

[7] This precessional motion ($\boldsymbol{F}$ and μ_F about $\boldsymbol{H}_0$) has a frequency of 10 to 30 kc in the Bureau standards, depending upon the magnitude of the C field. On the other hand, $\boldsymbol{\mu}$ can be pictured as precessing about $\boldsymbol{F}$ with a frequency of 9193 Mc.

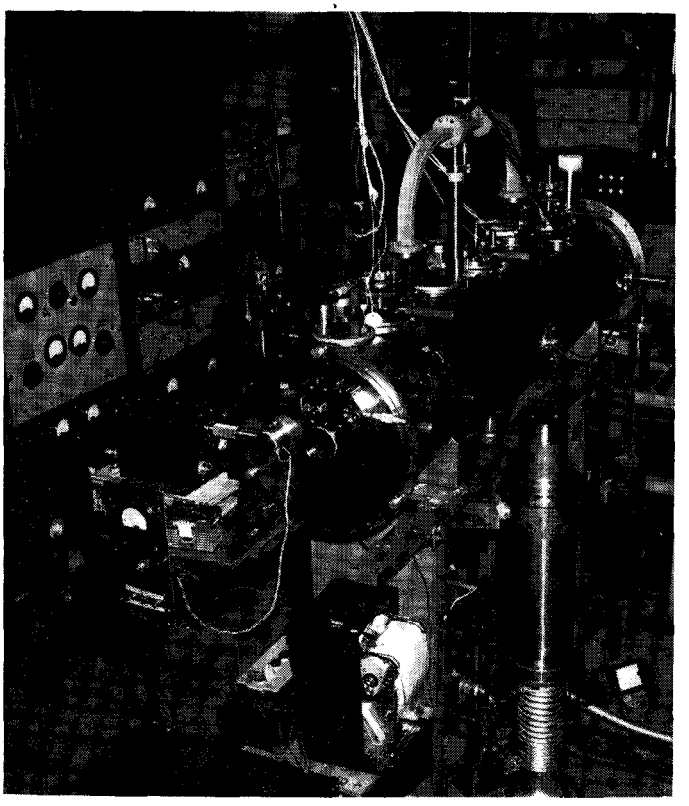

Fig. 5—(NBS-I) atomic beam frequency standard.

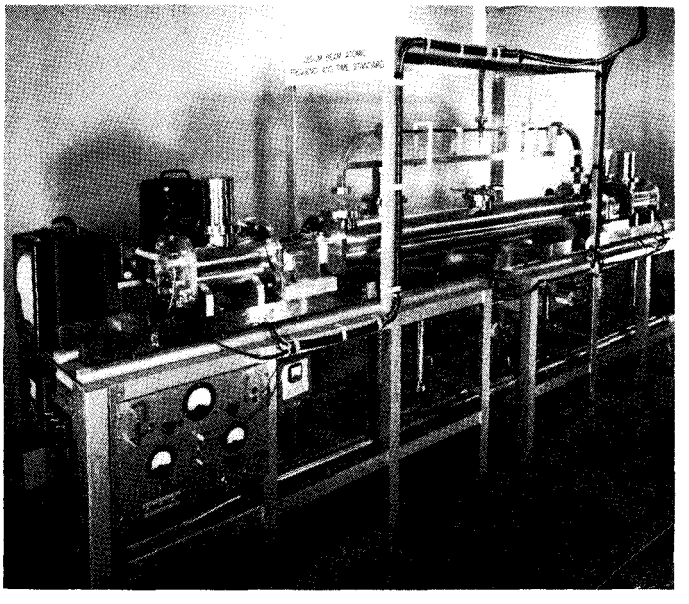

Fig. 6—(NBS-II) atomic beam frequency standard.

μ-metal magnetic shield. A double shield is used in the longer machine and a single shield in the shorter, to eliminate the earth's field.

The radiation field exciting the microwave transition is provided by a rectangular U-shaped resonant cavity driven by a frequency multiplier chain. The beam passes through the two ends of the cavity just grazing the end walls. The purpose of this design is to assure identical phase in the two oscillating field regions.

The cavity modes employed are $TE_{0,1,60}$ and $TE_{0,1,100}$ for NBS-I and NBS-II, respectively. The Q of both cavities is about 5000. The cavities were precisely electroformed to be symmetrical about the coupling hole to the transmission line from the frequency multiplier chain. Tuning is provided by a small plunger opposite the coupling hole.

The most recent method of frequency measurement is shown by the block diagram of Fig. 7.

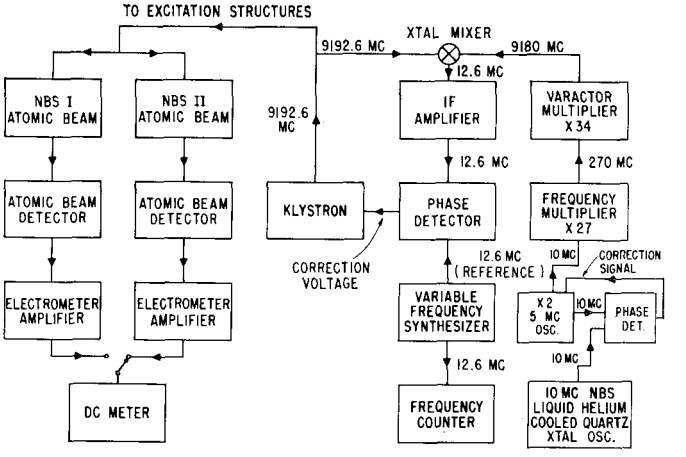

Fig. 7—Block diagram of the method of frequency comparison.

B. Effects Introducing Uncertainties in Frequency

There are a number of uncertainties introduced into the absolute frequency measurements of the cesium standard. The effects that we find to contribute most significantly to these uncertainties are:

1) the magnitude and nonuniformity of the C field including variations in the magnitude over long periods,
2) a phase difference between the two oscillating field regions, and
3) a lack of purity of the electromagnetic field exciting the atomic transition.

The magnitude of the C field is determined by observing a number of field sensitive microwave transitions, *e.g.*, $(F=4,\ m_F=\pm 1)\leftrightarrow(F=3,\ m_F=\pm 1)$. The frequency for these transitions is given by

$$\nu = \nu_0 \pm 700.6H_0,$$

where ν and ν_0 are measured in kc and H_0 in oersteds. The low-frequency transitions for which $\Delta F=0$ and $\Delta m_F=\pm 1$ were also used to measure the magnitude of the field and, in addition, the uniformity of the field. The frequency of these transitions is given by

$$\nu = 350H_0,$$

where ν is measured in kc. Small coils were placed at various positions along the C field. The magnitude and uniformity of H_0 were obtained by exciting each coil separately.

A rotating coil fluxmeter, sensitive to 0.002 oersted, provides still another method of measuring the field and its uniformity.

The initial field measurements made several months ago indicated that the maximum variation in H_0 along the length of the C field was ± 0.002 oersted, which was the uncertainty in the measurements at that time. This uncertainty in the field can produce, at most, an uncertainty in the standard frequency measurement given by

$$\Delta\nu_0' = 854 H_0 \Delta H_0;$$

$\Delta\nu_0' = 0.034$ cps if $H_0 = 0.020$ oersted. The fractional uncertainty is about 4×10^{-12}. At the time of these initial comparisons of the two standards, the values of the C-field magnitude, as measured by the different methods, agreed to within the precision of the measurements (± 0.002 oersted) for both machines. Since that time, however, the shielding properties of the μ-metal shields have deteriorated to some extent, accompanied, in the case of the longer machine, by a discrepancy among the various types of field measurements of about 0.004 oersted at a field of 0.080 oersted. In order to reduce the resulting uncertainty in the frequency measurements to below 1×10^{-11}, smaller C fields ($\sim$0.020 oersted) have been used in NBS-II for recent comparisons. There is no measurable discrepancy between the different C-field measurements in NBS-I.

In these field measurements, greatest reliability is placed in the microwave measurements. The spectral line measured at low frequencies is subject to distortion and power shifts. Furthermore, the line is at such a low frequency that the Bloch-Siegert shift is probably rather significant. The theory [6] assumes that H_1/H_0 (H_1 is the magnitude of the radiation field intensity) is a small number. The theory of Bloch and Siegert does not strictly apply to these experiments because $H_1/H_0 \sim 1$.

In order to test phase differences between the two oscillating field regions of the Ramsey exciting structure, the U-shaped cavities of both NBS-I and NBS-II were designed so that they can be rotated 180°; *i.e.*, the two oscillating fields can be interchanged. No frequency shift was observable after rotation of the long NBS-II cavity. A small shift of 1.0×10^{-11} was measured for NBS-I. The precision of measurement was 2×10^{-12}. Since the effect is doubled by rotating the cavity, the correction for the phase shift in NBS-I is 5×10^{-12}. It is supposed that this phase shift in NBS-I occurs as a result of extensive pitting on the inner wall of the cavity from improper electroforming. There is no pitting in the NBS-II cavity.

The simple theory of spectral line shape assumes the atomic transition to be excited by pure sinusoidal or cosinusoidal radiation.

If the electromagnetic field is not pure, rather large frequency uncertainties are possible in the measurements [7]. In actual fact, of course, the transition is induced by a certain distribution of frequencies. This distribution is determined by the frequency multiplier and crystal oscillator from which the exciting radiation is derived. The radiation, in general, is composed of the carrier frequency, noise, and discrete sidebands resulting from frequency modulation. The discrete sidebands are usually caused by 60 cps, the power frequency, and multiples thereof. (In the cesium beam experiments it is possible to reduce the noise to a low enough level so that it is not the limiting factor in the precision of the frequency measurements.) The sidebands are multiplied in intensity by the factor of frequency multiplication. This factor is rather large (1836) and, consequently, these sidebands can introduce rather large frequency errors. Errors of this sort are particularly significant if the power spectrum is unsymmetrical.[8] Frequency shifts of a few parts in 10^9 have been observed by deliberately introducing sidebands unsymmetrically placed about the carrier.

Of course, if the power spectrum is known, the proper spectral line shape can be calculated in order to find the proper correction to the measured frequency. It is more desirable, and much simpler, to eliminate these sidebands so that the simple line shape theory applies.

The frequency measurements of a few months ago were made by using a crystal oscillator whose crystal was cut to an exact submultiple of the cesium transition. The power spectrum of this oscillator was found to contain no observable sidebands by using an ammonia maser spectrum analyzer [9]. The half width of the power spectrum was about 5 cps at 23,900 Mc.

The measurement system now employs a helium cooled quartz oscillator. The power spectrum of this oscillator is shown in Fig. 8. The sidebands are eliminated by phase locking a simple two-tube oscillator to the helium oscillator. Thus, use is made of the short-term stability of the simple oscillator and the long-term stability of the more elaborate helium cooled oscillator. Any frequency uncertainty caused by the radiation spectrum should be negligible. A comparison of the data obtained, using the two methods of excitation, yield the same results within the precision of measurement.

Possible frequency shifts arising from neighboring lines in the spectrum have been estimated and were found to be negligible (see Fig. 9).

Frequency shifts incurred through frequency pulling of the resonant cavity are given approximately by

$$\Delta\nu_R = \left(\frac{Q_{\text{cavity}}}{Q_{\text{line}}}\right)^2 \Delta\nu_c,$$

where $\Delta\nu_R$ is the shift in the peak of the atomic resonance line, and $\Delta\nu_c$ is the difference in frequency between the peak of the cavity response and the peak of the spectral line. Q_{line} is the Q of the spectral line. Frequency shifts in the standard frequency measurements

[8] An unsymmetrical power spectrum can arise when the carrier is frequency modulated with two or more different frequencies [8].

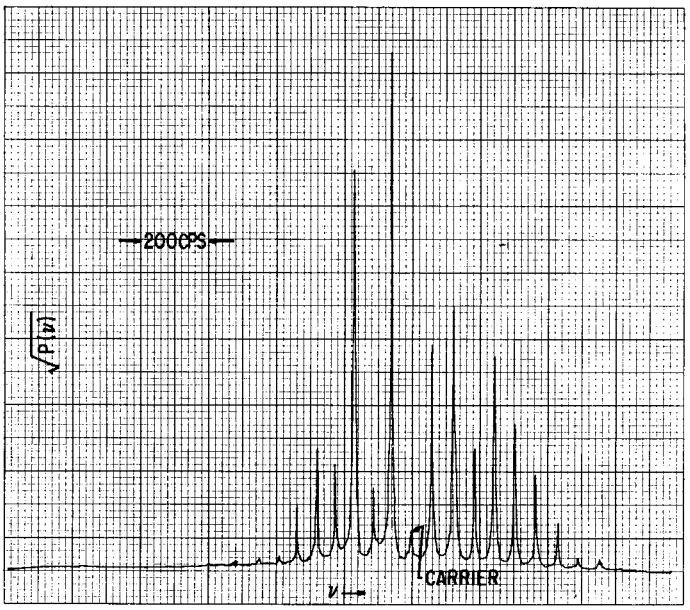

Fig. 8—The maser spectrum analyzer recording of the square root of the power spectrum of a frequency multiplier, chain driven by the helium cooled crystal oscillator. Multiplication factor = 2916. The sidebands are due to 60 cps and multiples of 60-cps FM.

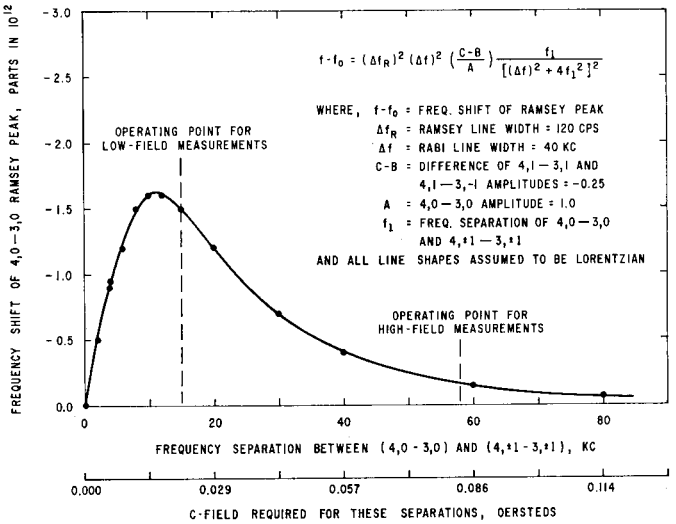

Fig. 9—Estimated shift of the NBS-II Ramsey peak due to nearby σ transitions of unequal amplitudes as a function of frequency separation.

from this source are found to be negligible, provided that reasonable care is taken in tuning the cavity to the cesium resonance. The cavity can be tuned to within 5 kc of this resonance. Temperature effects are not troublesome. The temperature of the laboratory is controlled within about 2°C. The cavity must be tuned to resonance not only to avoid frequency pulling effects, but also to avoid the phase shifts previously discussed.

The variation of the measured frequency as a function of excitation power has been examined experimentally. Changing the power by a factor of 10 introduces no observable frequency shift. (See Fig. 10.) Similar experiments have been performed on NBS-I, yielding similar results.

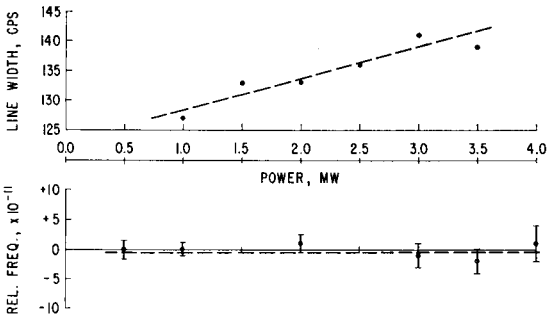

Fig. 10—Variation of resonance line width and frequency with power for NBS-II.

C. The Measurements

The accuracy of the frequency measurements is determined by consideration of the parameters of the beam devices that affect the frequency. The total uncertainty in frequency is obtained by adding all of the experimental uncertainties in these various measured parameters. A figure of accuracy can then be written for each of the two beams. If the beam devices are then compared, the difference frequency should fall within the sum of the two figures of accuracy and the precision of the comparisons.

The uncertainty in the C field for NBS-II is 0.004 oersted, and the corresponding frequency uncertainty is $\pm 8\times10^{-12}$. The uncertainty in the frequency caused by a phase shift between the oscillating fields is $\pm 2\times10^{-12}$. Other effects discussed previously are expected to be negligible, or calculable, and the corresponding uncertainty in frequency negligible. Thus, the figure of accuracy of NBS-II is 1.0×10^{-11}.

The uncertainty in the C-field measurements of NBS-I is ± 0.002 oersted or about 4×10^{-12}. The uncertainty caused by a phase shift is $\pm 2\times10^{-12}$, so that the figure of accuracy for NBS-I is 6×10^{-12}.

One would then expect that the two machines, if compared, would differ in frequency at most by 1.6×10^{-11} plus the precision of the comparison measurements.[9] This is the difference observed taking into account the phase shift of 5×10^{-12} in NBS-I. For one orientation of the NBS-I cavity the two devices disagree by 1.0×10^{-11} and for the other orientation they disagree by 2.0×10^{-11}. The corrected measured difference is 1.5×10^{-11}.

The precision for the comparisons considering the data over the last three months is 2×10^{-12}. Rather than adding this figure to the estimated figure of accuracy for each of the machines, the accuracy has been taken as 1.5×10^{-11}, the measured difference between NBS-I and NBS-II (a somewhat larger figure).

Confidence in these figures is gained by making the comparisons over long periods and observing the consistency. Also, various excitation sources were used. Certain modifications and adjustments and readjust-

[9] The measured phase shift in NBS-I (5×10^{-12}) and the shift caused by neighboring lines are not considered uncertainties since they are either measurable or calculable.

ments were made in order to observe the constancy of frequency measurements. Confidence is also gained from the observed statistical behavior. The randomness of the collected data was tested and found to follow a normal distribution. This gives additional meaning to the calculated standard deviation and standard deviation of the mean. The various sets of data taken for particular periods are found to agree within the standard deviation of the mean for each set.

The standard deviation is given by

$$\sigma = \frac{1}{\nu_0}\left[\frac{\sum_{i=1}^{n}(\nu_i - \bar{\nu})^2}{n-1}\right]^{1/2}, \tag{11}$$

if n comparisons are made between one beam and a particular crystal oscillator driving the frequency multiplier chain.

In comparing the two machines, the standard deviation is

$$\sigma' = \frac{1}{\nu_0}\left[\sum_{i=1}^{n}\frac{(\Delta\nu_i - \overline{\Delta\nu})^2}{n-1}\right]^{1/2}, \tag{12}$$

where $\Delta\nu_i$ is the measured zero field frequency difference between the standards. The standard deviations of the mean are given by

$$\sigma_M = \frac{1}{\nu_0}\left[\sum_{i=1}^{n}\frac{(\nu_i - \bar{\nu})^2}{n(n-1)}\right]^{1/2} \tag{13}$$

and

$$\sigma_M' = \frac{1}{\nu_0}\left[\sum_{i=1}^{n}\frac{(\Delta\nu_i - \overline{\Delta\nu})^2}{n(n-1)}\right]^{1/2}. \tag{14}$$

The number of sets of measurements is n. The time required to make a single comparison of one of the beams with a crystal oscillator is 30 seconds to 1 minute. The stability of this oscillator is of concern over the period of successive measurements. The measurements, in fact, give a good measure of the oscillator stability for these periods of time. Fig. 11 demonstrates the stability of the helium cooled oscillator. Actually, the instability displayed in this sample recording results from both instabilities in the maser and the crystal oscillator. The relative contributions are not distinguishable. Comparisons with the cesium beams frequently demonstrate a stability of 7 parts in 10^{12} for the helium oscillator over a period of a few hours. It is during these periods that the best comparisons between the two beams are made.

A set of 10 to 15 measurements taken over 5 to 15 minutes normally yields a standard deviation of the mean of 1×10^{-11}. Measurements are not made during periods of oscillator instability (when it is refilled with helium and so forth).

Fig. 12 shows a sample set of comparisons between NBS-I and NBS-II. The standard deviation of the mean of the comparisons for this day compares with a set of measurements made over a one-month period in January and February within the standard deviation of the mean. The oscillator was noticeably more unstable the last half of the day for the measurements made in Fig. 12.

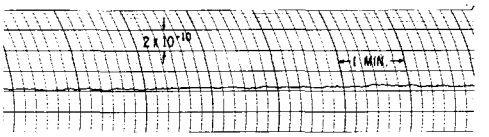

Fig. 11—Maser stabilized chain compared with 10-Mc helium cooled crystal oscillator. The recorder plots the analog output of a frequency counter vs time. The counting period is 1 second, and the display time is 1 second.

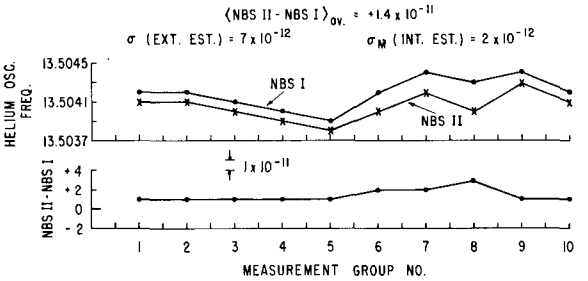

Fig. 12—NBS-II—NBS-I via helium cooled oscillator for one day's measurement (May 18, 1960).

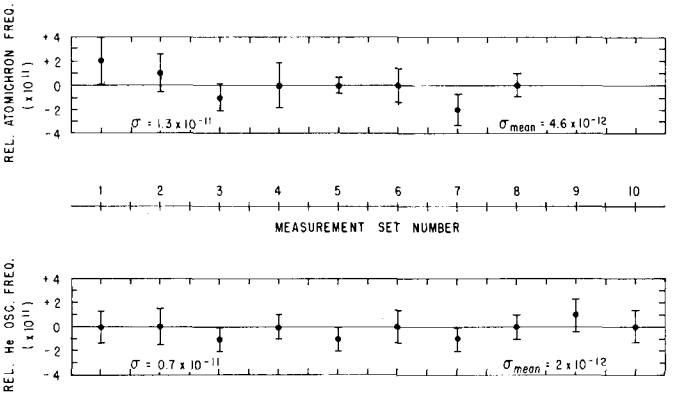

Fig. 13—Reproducibility of Atomichron and helium cooled oscillators. Comparisons during periods of eight hours.

Fig. 13 demonstrates the stability of Atomichron 106 and the helium cooled oscillator over eight-hour periods. These results are somewhat better than those observed typically.

V. Standard Frequency Comparisons With Other Cesium Standards

Comparisons have been made through propagation data between the Bureau standards, the British standard at the National Physical Laboratory, and four Atomichrons in the United States. The propagation data were obtained from the regular reports of: S. N. Kalra of the National Research Council of Canada; J. R. Pierce of the Cruft Laboratories; National Bureau of Standards Boulder Laboratories; Naval Research Laboratory, Washington, D. C.; and National Physical

TABLE I
SUMMARY OF THREE-MONTH COMPARISONS BETWEEN NBS-II AND NPL, NRC (CANADA), AND A GROUP OF 4 ATOMICHRONS
(DATA OF NOVEMBER 30, 1959–MARCH 1, 1960)

Comparison	Number of Daily Comparisons Used	Links Used in the Comparison
1) $(\text{NPL-NBS II})_{av.} = -0.1\times10^{-10}$ via NRC (Canada)	34	a. WWVB-NBS II b. WWVB-NRC c. MSF-NRC d. MSF-NPL
2) $(\text{NPL-NBS II})_{av.} = +0.9\times10^{-10}$	80	a. 106-NBS II b. WWV-106—(30 day averages) c. WWV-112 d. MSF-112 e. MSF-NPL
3) $(\text{NRC-NBS II})_{av.} = 10.2\times10^{-10}$	22	a. WWVB-NBS II b. WWVB-NRC
4) $(M_4\text{-NBS II})_{av.} = +1.0\times10^{-10}$ 106—Boulder 112—Cruft 109—WWV 110—NRL	70	a. WWV-106 b. 106-NBS II c. WWV-110 d. WWV-112 e. WWV-109

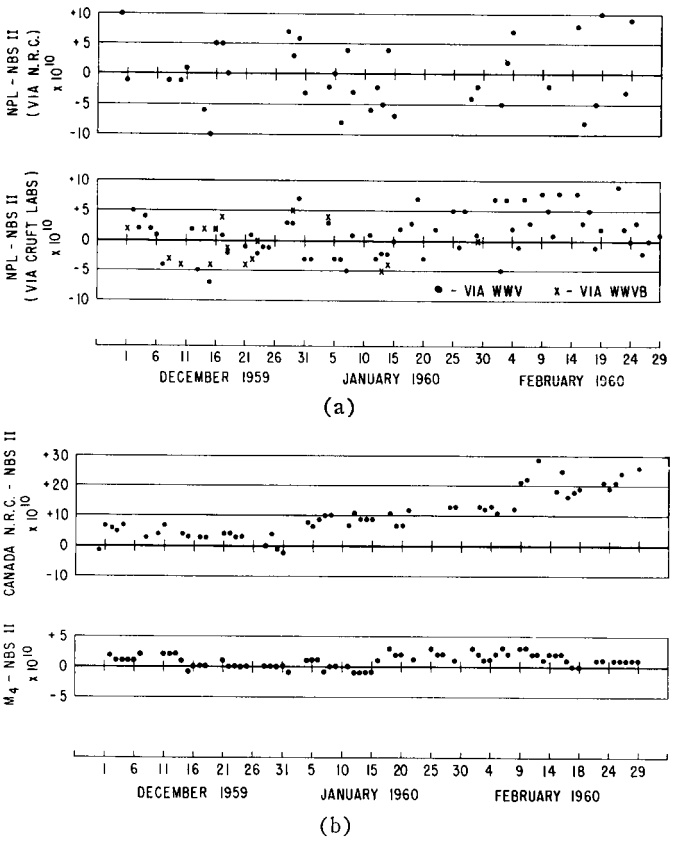

Fig. 14—(a) Comparison of U. S. frequency standard with British standard. (b) Comparison of U. S. frequency standard with Canadian standard, and with a group of four Atomichrons.

Laboratory, Teddington, England. The results are compiled in Table I. In this table, the designation M_4 is the mean of the zero field frequencies of Atomichrons 106, 109, 110, and 112. The locations of these Atomichrons are also indicated.

Fig. 14(a) and 14(b) plot the data used in Table I, and are given in order to display the scatter in the measurements.

VI. Discussion

The results of the experiments demonstrate that beam devices of rather modest length (55 cm between the oscillating fields) are capable of precisions of 2×10^{-12} for measurement times of about one to a few hours. Apparently, accuracies of 2×10^{-12} could also be obtained if the C-field difficulties that we have experienced could be eliminated. It seems likely that they can be. Longer beams would reduce the measuring time required for the same accuracy, provided that the C fields could be adequately controlled; longer beams would be accompanied by more severe C-field problems. Professor P. Kusch has suggested using Tl^{205} [1] instead of Cs^{133}. Thallium has the advantage that it is less sensitive (by a factor of 1/50) to magnetic fields. Its use could reduce the uncertainties in the determination of the line frequency. The transition frequency for thallium is given by

$$\nu_0'(\text{Tl}) = \nu_0(\text{Tl}) + 20.4H_0^2. \quad (15)$$

Compare this with cesium, for which

$$\nu_0'(\text{Cs}) = \nu_0(\text{Cs}) + 427H_0^2. \quad (2)$$

There are two additional advantages that the thallium spectrum has in precise frequency measurements: the σ transition has a higher frequency (21,310.835 Mc [10]) and it does not have other σ transitions as cesium does. There are only four states in the hyperfine structure of the ground state, and for cesium there are 16. Under these circumstances higher signal intensities would be observed for thallium if the detector efficiency were the same as for cesium. The disadvantage of thallium is that the method of detection is somewhat more difficult than the method used for cesium. The relative efficiencies must be determined by experiment before it can definitely be said that a thallium beam would provide a better standard.

The alkali vapor frequency standard [11], [12] also shows considerable promise although it has the disadvantage of inherent frequency shifts caused by the buffer gases. The shifts are not sufficiently understood to be treated analytically; consequently, certain recipes in construction would have to be prescribed if they were used as a primary standard. They do have certain advantages in simplicity, however. These devices have been demonstrated, by P. L. Bender and his group, to have frequency stabilities of 1×10^{-11} over a period of one month [13].

Hughes has suggested the $(J=0)\leftrightarrow(J=1)$ transition of Li^6F occurring at about 100 kMc as a frequency standard. It would employ the electric resonance beam technique [14]. A wider choice of frequencies is available in electric resonance beam experiments than in the atomic beam experiments. However, they have the disadvantage that signal intensities are lower.

It might be suggested that the Fabry-Perot interferometer, developed recently for the millimeter wave region [15], would be particularly well suited to this type of experiment. Q's of 100,000 are attainable and rather low-input powers can be used to excite the beam. The uniform C field could be provided by applying a voltage across the parallel Fabry-Perot plates. With presently available generators, and by using a Fabry-Perot resonator, it is perhaps not too optimistic to consider observing transitions at 500 kMc. There is the additional possibility of making a voltage standard from an electric resonance beam device employing a Fabry-Perot resonator.

The ammonia maser has application as a frequency standard [16]–[19] and, in fact, it is the present frequency standard of Switzerland.

Other masers designed for higher frequency are presently being investigated by a number of laboratories, including the Bureau. These devices employ a Fabry-Perot interferometer as the resonator. If these instruments prove to be practical, they will have the advantage of reducing the Doppler effect that exists in present ammonia masers.

The "bounce box" technique suggested by Ramsey [20] also shows promise in frequency standard applications. This device serves to store the atoms in the C-field region of an atomic beam spectrometer, thus decreasing the spectral line width.

At the present time, the National Bureau of Standards Boulder Laboratories intends to make a thallium beam, continue the research on the Fabry-Perot maser, and control the excitation chain of the present standards directly with an ammonia maser. It may prove practical to control the maser stabilized chain controlling the cesium excitation with a correction signal from the cesium beam. Thus, the complete standard would be composed of an ammonia maser that would provide short-term stability and the cesium beam which would determine the long-term stability.

VII. Concluding Remarks

The longer of the two machines (NBS-II) is the present United States Frequency Standard. The shorter machine (NBS-I) is an alternate standard. The frequency assumed for the $(F=4,\ m_F=0)\leftrightarrow(F=3,\ m_F=0)$ transition of cesium in zero field is 9,192,631,770.0 cps. At present, the best comparison between cesium and Ephemeris Time is that given by Markowitz, Hall, Essen and Parry as $9{,}192{,}631{,}770\pm20$ cps [21].

Corrections for the 60-kc standard frequency broadcasts of Station WWVB (formerly KK2XEI), Boulder, Colo., are made each week and are available upon request. The corrections for the 20-kc transmission are also available.

We believe that the experiments demonstrate that with adequate care in construction and testing, atomic beam standards can be expected to agree in frequency without special recipes in design, and indeed they behave as one would predict from theory; one need only know the values of the pertinent parameters to sufficient accuracy. This information must be obtained from appropriate tests.

VIII. Acknowledgment

The authors wish to acknowledge the invaluable assistance of J. Barnes and Dr. G. Schafer, who contributed significantly to a number of the electronic problems, and H. Salazar who built most of the electronic equipment. We wish to recognize the help of L. Fey in the initial stages of this research. The beam devices were built in the Bureau Instrument Shop. Thanks are especially due J. Carlson, D. Harriman, D. Penner, and V. Schmitz. The helium cooled oscillator employed in these experiments was designed by A. H. Morgan of the Broadcast Services Section of the Bureau. The quartz crystal itself was fabricated by the Bell Telephone Laboratories. The authors also wish to express their thanks to Dr. A. V. Astin for his continued interest, support and aid.

Bibliography

[1] P. Kusch, "Precision atomic beam techniques," *Proc 11th Annual Frequency Control Symp.*, U. S. Army Signal Res. and Dev. Lab., Fort Monmouth, N. J., pp. 373–384; May, 1957.
[2] J. Holloway, W. Mainberger, F. H. Reder, G. M. R. Winkler, L. Essen, and J. V. L. Parry, "Comparison and evaluation of cesium atomic beam frequency standards," Proc. IRE, vol. 47, pp. 1730–1736; October, 1959.
[3] A. O. McCoubrey, "Results of the comparison: Atomichron—British cesium beam standard," IRE Trans. on Instrumentation, vol. I-7, pp. 203–206; December, 1958.
[4] R. C. Mockler, R. E. Beehler, and J. A. Barnes, "An evaluation of a cesium beam frequency standard," in "Quantum Electronics—A Symposium," C. H. Townes, Ed., Columbia University Press, New York, N. Y., pp. 127–145; 1960.
[5] P. Kusch and V. W. Hughes, "Atomic and molecular beam spectroscopy," in "Encyclopedia of Physics," S. Flügge, Ed., Springer, Berlin, pp. 1–172; 1959.
N. F. Ramsey, "Molecular Beams," Oxford University Press, London, Eng.; 1956.
H. Kopfermann, "Nuclear Moments," Academic Press, New York, N. Y.; 1958.
[6] F. Bloch and A. Siegert, "Magnetic resonance for nonrotating fields," *Phys. Rev.*, vol. 57, pp. 522–528; March, 1940.
[7] N. F. Ramsey, "Shapes of molecular beam resonances," "Recent Research in Molecular Beams," I. Estermann, Academic Press, New York, N. Y., pp. 107–119; 1959.
[8] H. S. Black, "Modulation Theory," D. Van Nostrand Co., New York, N. Y., pp. 195–200; 1953.
[9] J. A. Barnes and L. E. Heim, "A High Resolution Ammonia Maser Spectrum Analyser," to be published.
[10] A. Lurio and A. G. Prodell, "Hfs separations and Hfs anomalies in the $^2P_{1/2}$ state of Ga^{69}, Ga^{71}, Tl^{203}, and Tl^{205}," *Phys. Rev.*, vol. 101, pp. 79–84; January, 1956.
[11] P. L. Bender, "Atomic frequency standards and clocks," in "Quantum Electronics—A Symposium," C. H. Townes, Ed.,

Columbia University Press, New York, N. Y., pp. 110–121; 1960. Additional references are given.
[12] C. O. Alley, "Coherent pulse technique in the optical detection of the 0↔0 ground state hyperfine resonance in rubidium 87," in "Quantum Electronics—a Symposium," C. H. Townes, Ed., Columbia University Press, New York, N. Y., pp. 146–156; 1960.
[13] R. J. Carpenter, E. C. Beatty, P. L. Bender, S. Saito, and R. O. Stone, "A prototype rubidium vapor frequency standard," this issue, p. 132.
[14] V. W. Hughes, "Considerations on the design of a molecular frequency standard based on the molecular beam electric resonance method," *Rev. Sci. Instr.*, vol. 30, pp. 689–694; August, 1959.
[15] W. Culshaw, "High resolution millimeter wave Fabry-Perot interferometer," IRE TRANS. ON MICROWAVE THEORY AND TECHNIQUES, vol. MTT-8, pp. 182–189; March, 1960.
[16] J. P. Gordon, H. Zeiger, and C. H. Townes, "Maser—new type of microwave amplifier, frequency standard, and spectrometer," *Phys. Rev.*, vol. 99, pp. 1264–1274; August, 1955.
[17] J. Bonanomi and J. Herrmann, "Determination of the ammonia inversion frequency," *Helv. Phys. Acta*, vol. 29, pp. 451–452; 1956.
[18] R. C. Mockler, J. A. Barnes, R. E. Beehler, and R. L. Fey, "The ammonia maser as an atomic frequency and time standard," IRE TRANS. ON INSTRUMENTATION, vol. I-7, pp. 201–202; December, 1958.
[19] S. Hopfer, "Performance of a maser frequency standard," *Proc. 14th Annual Frequency Control Symp.*, U. S. Army Signal Res. and Dev. Lab., Fort Monmouth, N. J.; June, 1960. To be published.
[20] D. Kleppner, N. F. Ramsey, and P. Fjelstadt, "Broken atomic beam resonance experiment," *Phys. Rev. Lett.*, vol. 1, pp. 232–233; October, 1958.
[21] W. Markowitz, R. G. Hall, L. Essen, and J. V. L. Parry, "Frequency of cesium in terms of ephemeris time," *Phys. Rev. Lett.*, vol. 1, pp. 105–107; August, 1958.
L. Essen and J. V. L. Perry, "The caesium resonator as a standard of frequency and time," *Phil. Trans. Royal Soc. (London) A*, vol. 250, pp. 45–69; August, 1957.